JOURNAL OF MATERIALS SCIENCE 28 (1993) 4892–4899

Effect of pre- and post-weld heat treatments on the mechanical properties of electron beam welded Ti–6Al–4V alloy

G. THOMAS, V. RAMACHANDRA, R. GANESHAN
Vikram Sarabhai Space Centre, Trivandrum, India

R. VASUDEVAN
Department of Metallurgical Engineering, Indian Institute of Technology, Madras, India

This paper represents a summary of experimental work carried out to find the effect of various pre- and post-weld heat treatments on Ti–6Al–4V alloy. In the as-welded state the samples exhibit about 80% of the tensile ductility and about 90-95% of the impact/fracture toughness of the base metal. Low temperature stress relieving or ageing carried out subsequent to the welding operation improves the tensile properties but decreases the toughness at the fusion zone. Solution treatment followed by welding and ageing or the post-weld solution treatment and ageing treatment leads to only a marginal increase in tensile strength at the expense of toughness at the fusion zone. High temperature annealing of the welded samples does not increase the tensile ductility but improves the toughness at both the fusion zone and the heat affected zone. The above facts and a special burst-pressure test conducted on a gas bottle in the as-EB welded state show that Ti–6Al–4V components can be used without subjecting them to any post-weld heat treatments.

1. Introduction

The unique combination of high specific strength, high temperature capability, good corrosion resistance to most fuels and oxidizers, good fracture toughness and good fabricability has established Ti–6Al–4V alloy as a potential material for aerospace applications [1]. This alloy is used in the Indian Space Programme as the material for gas bottles, the reaction control system tanks and the fuel and oxidizer tanks. Electron beam welding (EBW) is used as the joining process for these components which demand maximum weld quality and high reliability in service. As experience in EBW of this alloy is limited in India, a programme was initiated with the following objectives.

1. To study the effect of electron beam welding parameters on the depth of penetration.
2. To determine the effect of pre- and post-weld heat treatments on the mechanical properties and microstructures of the EB welded joints.

The first part of this work was carried out using 25 mm thick Ti–6Al–4V sections and the findings have been reported elsewhere [2]. In the second part of the work, EB welded joints were evaluated for their mechanical properties in the as-welded as well as in various heat treated conditions. In general the welds in α-β titanium alloys exhibit increased strength and decreased ductility as compared to the base metal (BM). The decrease in weld ductility increases with increasing quantities of β stabilizing elements and it is overcome, at least partially, by altering the welding parameters and cooling rates and by the use of chemically dissimilar filler wires [3–6]. The fact that the use of dissimilar filler metal does not alter the chemistry of the heat affected zone (HAZ) restricts its usefulness. Therefore post-weld heat treatments which bring about a change in the microstructure of the fusion zone (FZ) and HAZ are used as an important method for restoring the lost ductility of the welded material. Earlier investigations [7–11] in this area have mostly been limited to post-weld treatments, like annealing, stress relieving and triplex annealing. In this study the following combinations of heat treatments have been carried out to find their effect on the properties of welded material.

1. As received (annealed) + welded (condition A)
2. As received + welded + stress relieved (condition B)
3. As received + solution treated + welded + aged (condition C)
4. As received + welded + solution treated + aged (condition D)
5. As received + welded + annealed (condition E)

The effect of these treatments on weldments has been determined through tensile, impact and fracture toughness tests, measurements of microhardness variation across weldments and metallographic and fractographic studies.

2. Experimental procedure

The experimental and testing procedures adopted for this study are given in detail elsewhere [12].

0022–2461

2.1. The machine

The electron beam welding was carried out in a 12 kW capacity, 150 kV Hawker Siddeley machine at the Gas Turbine Research Establishment (GTRE), Bangalore, India.

2.2. Material

In this study hot rolled and annealed plates of 20 mm thickness (M/S Enpar, UK) were used. The chemical composition of the plate is given in Table I.

2.3. EBW conditions

The best welding conditions, arrived at for a single pass square butt joint by examining the top and bottom bead appearance, studying the internal soundness through radiographic tests and determining the mechanical properties through tensile tests, are given in Table II.

2.4. Pre- and post-weld heat treatments

The annealed plate was cut into $60 \times 60 \times 20$ mm pieces and some of the pieces were given a solution treatment prior to welding. Similarly, some of the welded joints were subjected to various post-weld treatments. The heat treatments were done in air and the oxide layer formed on the surfaces was removed by milling. Annealing consisted of holding at 950 °C for 2 h followed by air cooling. Stress relieving was carried out at 540 °C for 2 h followed by air cooling. Solution treatment consisted of holding at 950 °C for 2 h followed by water quenching. Ageing was performed at 540 °C for 2 h followed by air cooling.

2.5. Sample preparation and testing

The samples for the various tests were prepared from welded joints found to be radiographically sound as per the ASME pressure vessel code [13]. The tensile test samples were prepared from the welded plates with the weld line at the centre of the gauge length. In the case of Charpy V-notch and fracture toughness specimens care was taken to locate the V-notch at the centre of the FZ or the HAZ to measure the toughness at the respective zone. Fig. 1 shows the location of the weld line in various test samples. The fracture toughness tests were performed on compact tension specimens of 16 mm thickness prepared as per the standard ASTM E-399-87. The specimens were pre-cracked and opened out in an Instron Model 8033 servohydraulic machine. The fractured surfaces of the impact samples were observed in a scanning electron microscope (SEM) for their surface topography.

TABLE I Chemical composition of Ti–6Al–4V plate

Element	C	Al	V	Fe	O	N	H	Ti
wt %	0.028	6.13	3.89	0.20	0.16	0.02	0.004	Balance

TABLE II Optimized EBW parameters for 20 mm thick Ti–6Al–4V alloy

Accelerating voltage	150 kV
Beam current	70 mA
Travel speed	150 cm min^{-1}
Gun-to-work distance	190 mm
Beam focus	25 mm below the surface
Chamber pressure	1.333×10^{-2} Pa

3. Results

The ultimate tensile strength (UTS), the yield strength (YS), the percentage elongation (%E) and the percentage reduction in area (%RA) values obtained from the tensile tests and the Charpy V-notch impact and the fracture toughness values for the base metal and welded samples under various conditions are summarized in Table III.

3.1. Tensile properties

A comparison of the UTS, YS and %E values of the base metal and the welded samples under various conditions are given in Fig. 2. While the reduction in UTS is not appreciable the YS and the %E values of sample A are found to decrease from 990 MPa and 16% (values of the base metal in the annealed condition) to 910 MPa and 12.6%, respectively. The weld efficiency of sample A in terms of UTS is about 95%, while it is only 90% in terms of YS. The UTS and YS values of sample B are around 8% and 13%, respectively, higher than those of sample A. If sample C shows around 9–10% reduction in UTS and YS values as compared to those of the base metal in the solution treated and aged (STA) condition, it shows an increase of about 5% in UTS and 10% in YS values as compared to those values of sample A. The UTS and YS values of sample C are seen to be only slightly (around 3%) lower than those of sample B. However, both samples B and C exhibit higher tensile ductility than that of sample A. Sample D possesses around 14% higher UTS and YS values as compared to those

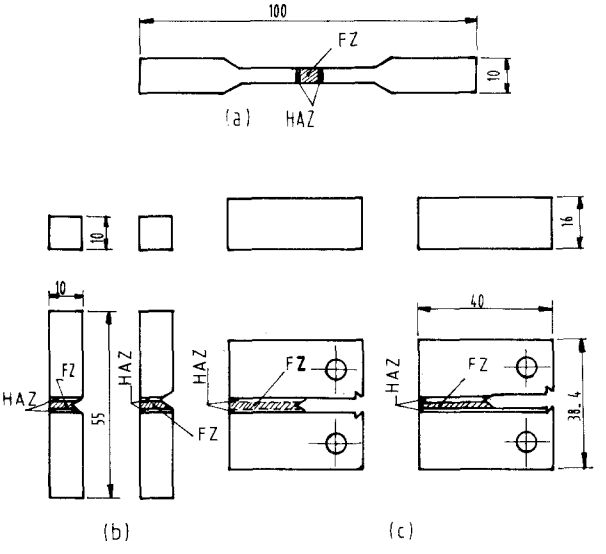

Figure 1 Location of the weld in the tensile, impact and fracture toughness testing samples.

TABLE III Average mechanical properties of base metal and EB welded joints in various conditions

Condition		Tensile properties				Impact toughness (J)			Fracture toughness (MPa $m^{1/2}$)		
		UTS (MPa)	YS (MPa)	%E (25 mm GL)	%RA	PM	HAZ	FZ	PM	HAZ	FZ
O	Parent metal (annealed)	1039.5	990.5	16.0	49	19.6			60.5		
S	Parent metal (solution treated)	1059.0	1029.7	15.0	48	20.0					
STA	Parent metal (STA)	1176.8	1093.5	10.5	47	18.0			52.0		
A	Annealed + welded	1006.2	910.0	12.6	47		20.5	18.8		58.0	55.5
B	Annealed + welded + stress relived	1085.6	1024.8	15.0	43		20.4	15.3		55.8	45.0
C	Solution treated + welded + aged	1052.3	997.3	13.6	46		19.6	14.1		55.0	44.5
D	Annealed + welded + STA	1147.4	1039.5	8.3	43		21.9	16.5		56.0	49.5
E	Annealed + welded + annealed	993.5	925.0	12.7	46		23.5	22.0		69.0	67.3

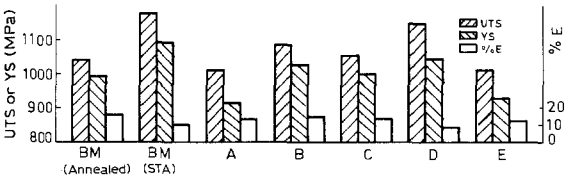

Figure 2 A comparison of tensile properties of base metal and EB welded samples in various conditions.

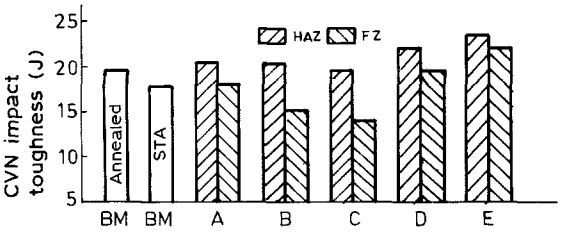

Figure 3 A comparison of impact toughness values of base metal and EB welded samples in various conditions.

values of sample A. Sample D also has higher UTS and YS values than those of sample C, but slightly lower values than those of the base metal in the STA condition. However, the tensile ductility of sample D is seen to be the minimum of all conditions. The tensile properties of sample E are comparable to those of sample A, but are lower than those of the base metal in the annealed condition.

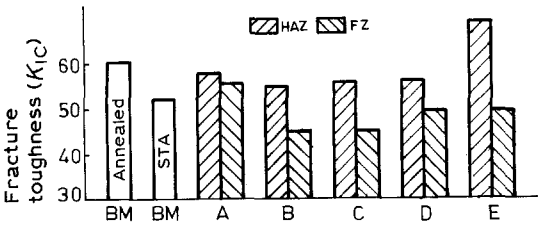

Figure 4 A comparison of fracture toughness values of base metal and EB welded samples in various conditions.

3.2. Impact/fracture toughness

The impact toughness and the fracture toughness values for the welded samples at the FZ and HAZ and those for the base metal under different conditions are compared in the form of bar charts in Figs 3 and 4, respectively.

From Fig. 3 it can be seen that the impact toughness of sample A at the FZ is about 95% that of the base metal in the annealed condition. The impact toughness at the FZ of sample B is about 18% less than that of sample A. Sample C represents the condition of minimum FZ impact toughness of all the pre- and post-weld heat treated conditions. The FZ impact toughness of sample D is lower (about 12%) than that of sample A, but comparable to the impact toughness of the base metal in the STA condition. Sample E represents the maximum FZ impact toughness of all conditions. It is about 12% more than the impact toughness of the base metal in the annealed condition and about 15% more than that of sample A. In Fig. 3 it can also be seen that the HAZ impact toughness in all cases is equal to or greater than the impact toughness of the base metal in the annealed condition, indicating that neither the welding operation nor the post-weld heat treatments tend to deteriorate the impact toughness at the HAZ. In fact, the impact toughness value at the HAZ of sample E is 20% more than the impact toughness of the base metal in the annealed condition.

Fig. 4 shows that the fracture toughness values also follow the same trend as the impact toughness in almost all cases. The fracture toughness of sample A is about 90% at the FZ and about 95% at the HAZ as compared to the fracture toughness value of the base metal in the annealed condition. As in the case of impact toughness, samples B, C and D have low FZ fracture toughness. Sample C represents the condition of minimum FZ and HAZ fracture toughness and sample E represents the condition of maximum FZ and HAZ fracture toughness. The FZ fracture toughness of sample E is about 21% more than that of

sample A and about 11% more than the fracture toughness of the base metal in the annealed condition.

4. Discussion

Sample A in the as-welded state shows a reduction of 5–10% in the FZ impact/fracture toughness as compared to the base metal values in the annealed condition. The microhardness plot (Fig. 5a) across the weld joint of sample A shows that the hardness across the FZ is relatively higher than in the case of the base metal. The FZ of sample A has an average microhardness of 420 VPN, as compared to that of 390 VPN for the base metal. This observation of higher hardness at the FZ of sample A is in agreement with the earlier observation of a slightly reduced FZ impact/fracture toughness and a lower tensile ductility. Fig. 6 shows the microstructure of the base metal and the HAZ of sample A. The microstructure of the base metal reveals the presence of equiaxed primary α in a matrix of transformed β. The microstructure of the HAZ of sample A contains equiaxial α, acicular α and short martensite phases. The microstructure of the FZ of sample A (Fig. 7) consists predominantly of

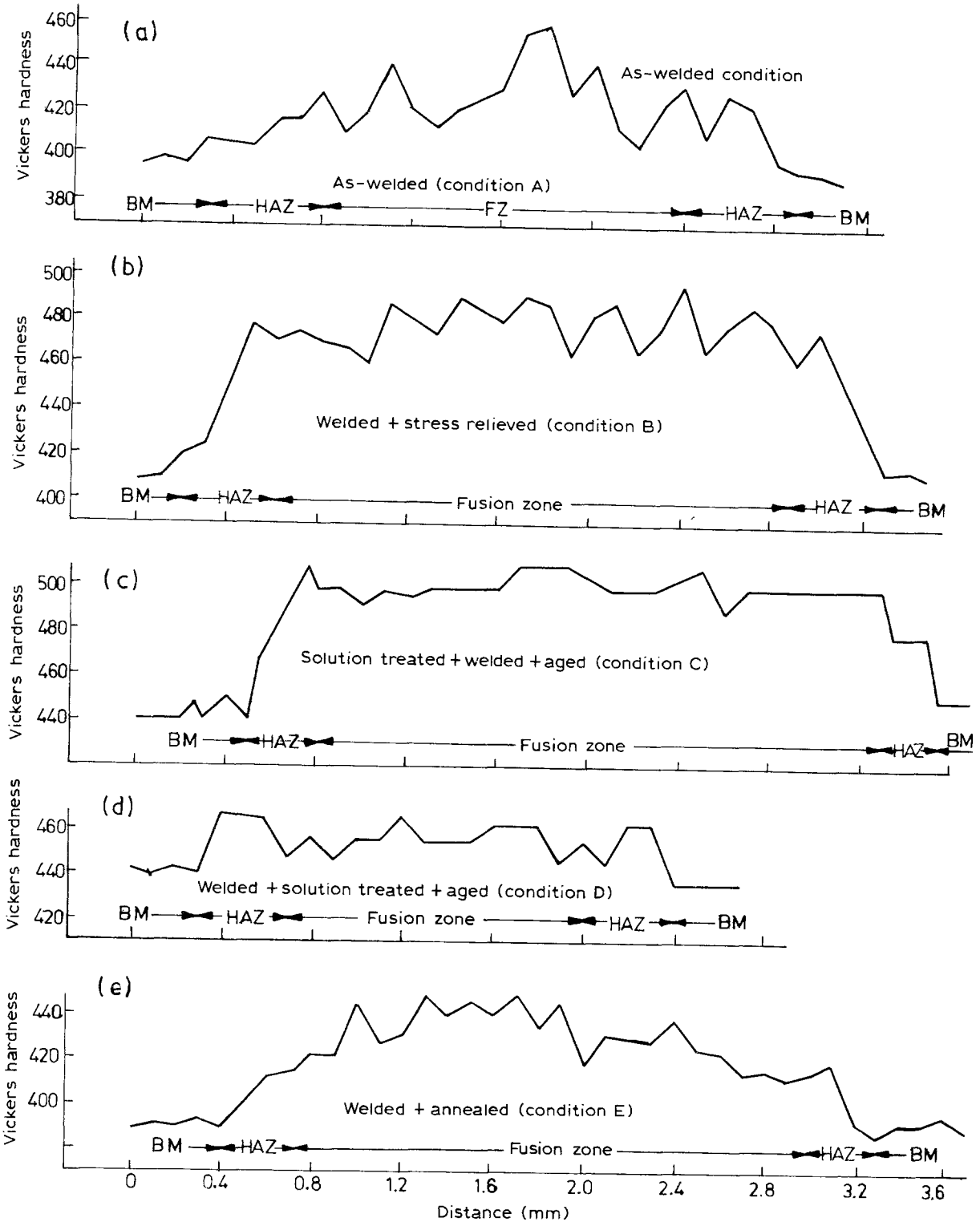

Figure 5 Variation of microhardness across the welded samples subjected to various pre- and post-weld heat treatments.

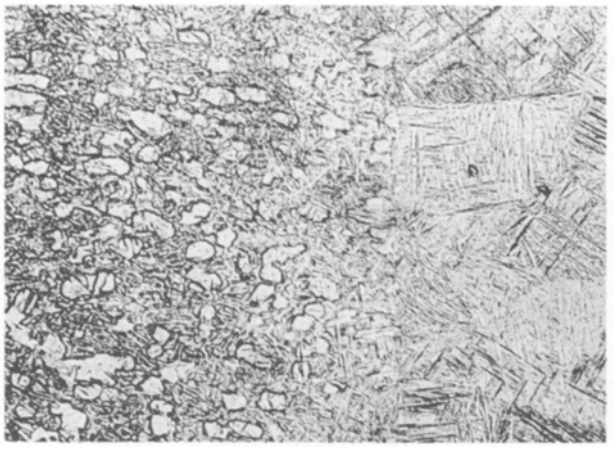

Figure 6 Microstructure (320 ×) of base metal and HAZ of sample A.

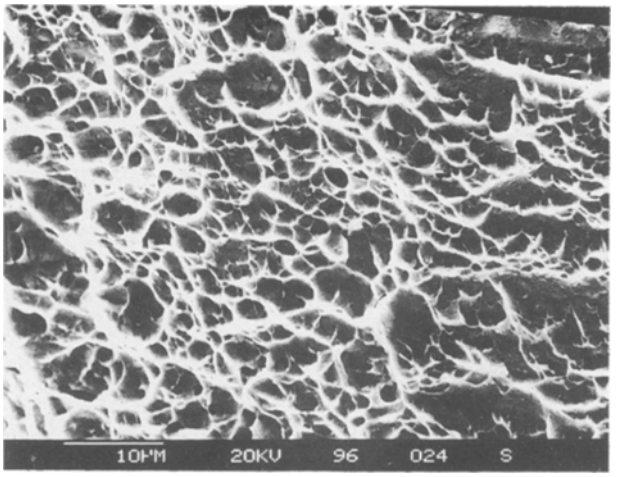

Figure 8 Fractograph of base metal in the annealed condition.

Figure 7 Microstructure (320 ×) of FZ of sample A.

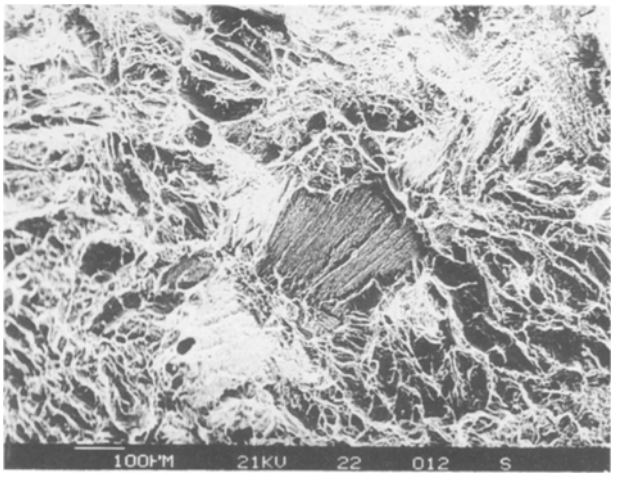

Figure 9 Fractograph of FZ of sample A.

long narrow martensitic needles. Though there is an apparent reduction in impact/fracture toughness and increase in hardness at the FZ of sample A, it can be said that they are inappreciable. This is reflected in the ductile fractograph of the FZ of sample A. The fractograph of the base metal (Fig. 8) in the annealed condition and that of the FZ of sample A (Fig. 9) show a dimpled appearance, indicating that the fracture mechanism is one of microvoid coalescence in both cases.

Although sample A in the as-welded condition retains almost 90–95% of the impact/fracture toughness of the base metal in the annealed condition, the low temperature post-weld heat treatments, like stress relieving and ageing (samples B and C), bring about a deterioration in the impact/fracture toughness of the FZ. The hardness measurements across the FZs of samples B and C (Fig. 5b and c) also show a comparatively higher hardness than that across the FZ of sample A. The microstructures of FZ of samples B and C are almost similar and they reveal the presence of tempered martensite (Fig. 10). The FZ fractograph of these samples are also almost identical and reveal regions of brittle fracture (Fig. 11). The observation of a brittle type of fracture in samples B and C is in agreement with the lower FZ impact and fracture toughness values and the higher microhardness at the FZ of these samples. However, the transmission electron microscopic structure of solution treated and

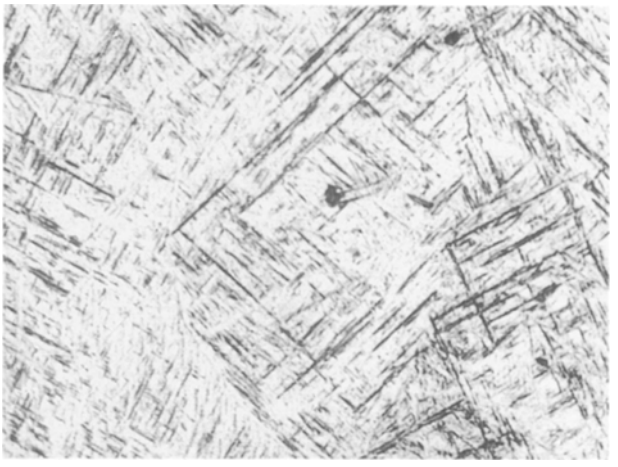

Figure 10 Microstructure (320 ×) of FZ of sample B.

aged Ti–6Al–4V alloy presented by Chestnut [14] clearly shows the formation of irregular shaped or ellipsoidal β precipitate in the tempered martensite. The strong tempered martensite produced at the FZs of samples B and C by the post-weld ageing or tempering does not retard unstable crack propagation by allowing localized yield. Thus we find the impact and fracture toughness of these samples reduced to a

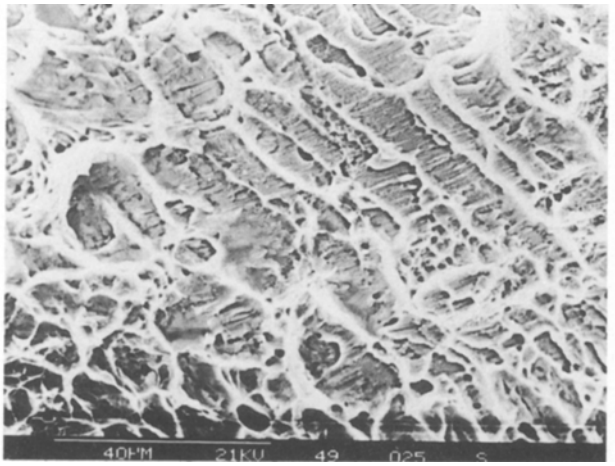

Figure 11 Fractograph of FZ of sample B.

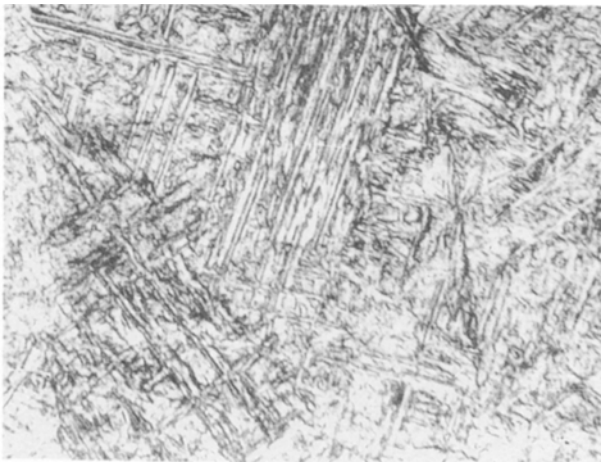

Figure 12 Microstructure (320×) of FZ of sample D.

minimum. However, it is interesting to note that these samples exhibit higher tensile elongation than that of sample A. The fractographs of the HAZ of these samples are similar to that of the fractograph of the base metal.

The microstructure (Fig. 12) of the FZ of sample D does not reveal the presence of any tempered martensite. It consists mainly of the acicular α with β phase present at the α–α interface. The fractographs of the FZ and HAZ of sample D show a dimpled appearance and are similar to those of sample A. The microhardness plot (Fig. 5d) of sample D shows a higher hardness across its FZ as compared to that across the base metal, even after the post-weld solution and ageing treatments.

The post-weld annealing operation carried out in the case of sample E has led to a coarsening of the acicular α and the formation of grain boundary α (Fig. 13). When the propagating crack encounters the grain boundary α, it finds a site where its stresses can readily be relieved by plastic flow. This would make the crack tip blunt and a higher stress would be required to propagate the crack further. This is clear from the fractograph of the FZ of sample E (Fig. 14), which reveals extensive crack branching around prior β grains. The higher impact and fracture toughness values of the post-weld annealed sample E are attributed to the microstructural changes taking place during annealing. Like sample D, sample E also shows a relatively higher microhardness value at the FZ as compared to that of the base metal, even after the post-weld annealing operation. This higher hardness at the FZs of all the samples may result from the basic weld structure, which is not completely altered in the post-weld heat treatments. The microstructure (Fig. 15) of the HAZ of sample E also reveals coarse, short acicular α and grain boundary α.

The impact and fracture toughness values at the HAZ of all the samples are seen to be always greater than their respective FZ values. The higher impact/-fracture toughness values at the HAZ results from the sum total of the various microstructural changes that take place at the HAZ at the time of welding and during the post-weld heat treatments. Regions of HAZ

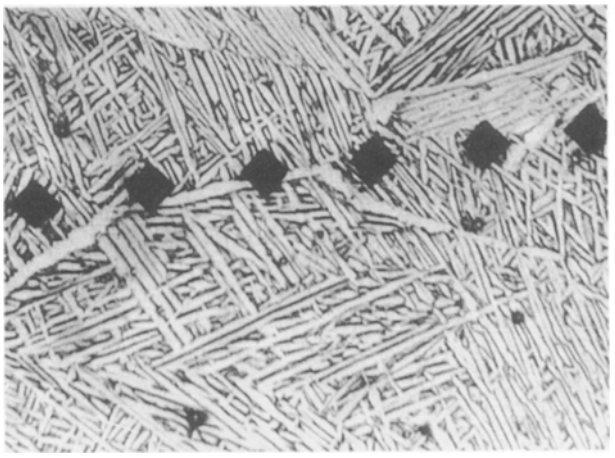

Figure 13 Microstructure (320×) of FZ of sample E.

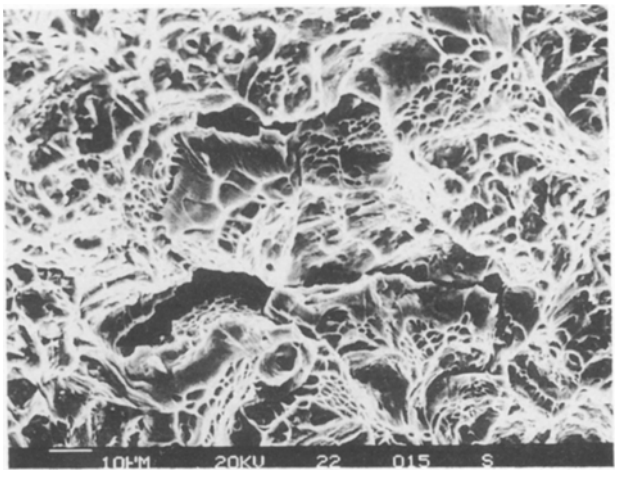

Figure 14 Fractograph of FZ of sample E.

which are far from the FZ are heated to relatively low temperatures. The microstructure of this region is almost the same as that of the base metal and the impact toughness of this region of HAZ will correspond to that of the base metal. The regions of HAZ which are close to FZ are heated to very high temperatures and their microstructure will contain predominantly martensite, as in Fig. 7. Hence the

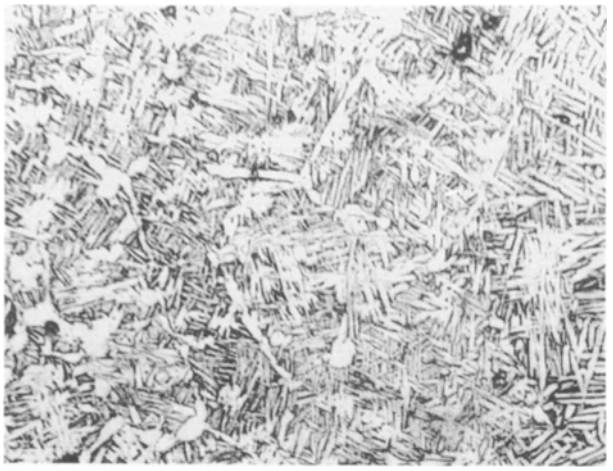

Figure 15 Microstructure (320×) of HAZ of sample E.

impact/fracture toughness values of this region will correspond to that of the FZ. The middle region of the HAZ, which is heated to temperatures slightly above the β transus and where the cooling rate is relatively slow, contains mainly acicular α, which is known for its higher toughness. The subsequent low temperature post-weld heat treatments adversely affect the impact/fracture toughness of only a small region of HAZ lying close to the FZ. Hence the average impact/fracture toughness of the HAZ of these samples are slightly lower than that of the base metal or always higher than that of their FZs. The high temperature post-weld annealing treatments favourably contribute to the impact/fracture toughness of the middle region, as well as the region of the HAZ lying close to FZ through microstructural changes. The presence of coarse and short acicular α in the HAZ of sample E may be responsible for the higher impact/fracture toughness of this zone.

4.1. Tensile ductility

While sample A shows a reduction in tensile ductility with attendant decrease of tensile strength, samples B and C exhibit an increase in tensile ductility accompanied by an increase in tensile strength and a decrease in impact/fracture toughness as compared to sample A. A similar situation of high tensile ductility and low fracture toughness is reported by Simpson [15] in the case of synthetically produced HAZ of Ti–6Al–6V–2Sn alloy. Although sample D shows the minimum tensile ductility, it is comparable to that of the base metal in the STA condition. Sample E does not show any noticeable improvement in tensile ductility on post-weld annealing. The annealing carried out by Vaughan [7] on 10 mm thick, EB welded Ti–6Al–4V joints at 720 °C for 1 h followed by air cooling did not increase its tensile elongation from 12% of the value of the as-welded condition but slightly decreased the fracture toughness (K_Q) from 67.2 to 63.7 MPa $m^{1/2}$. In this case the time and temperature of annealing do not seem to be sufficient enough to effect any coarsening of the α phase or the formation of grain boundary α, as in the case of sample E. Gurevich *et al.* [15] have reported an improvement in tensile elongation from 7.5 to 12.6% and fracture toughness from 80.6 to 110.7 MPa $m^{1/2}$ on a 55 mm thick, EB welded Ti–6Al–4V sample subjected to vacuum annealing at 750 °C for 48 h. The long duration of annealing in vacuum would have been sufficient to cause coarsening of the α phase and the formation of grain boundary α resulting in a higher fracture toughness value. The increase in elongation noticed in this case might have resulted mainly from the removal of gaseous impurities, like hydrogen, and the elimination or redistribution of inclusions in the weld, since the present study has shown that the coarsening of the α phase and the formation of grain boundary α do not increase the tensile elongation but only the impact/fracture toughness.

4.2. Evaluation of the conditions

In the case of sample A it can be seen that it retains at the FZ almost 90–95% of the impact/fracture toughness and 85% of the tensile ductility of the base metal in the annealed condition. From the low FZ impact/fracture toughness values of samples B and C (70–80% of the base metal in the annealed condition) it appears that the post-weld stress relieving or the costly and difficult step of solution treating the sample prior to welding followed by post-weld ageing are superfluous. In the case of sample D the 5–10% increase in UTS and YS strength obtained by the post-weld solution treatment and ageing is nullified by the 16–18% decrease in the FZ impact/fracture toughness when compared to sample A. While an increase of a little over 20% in FZ fracture toughness might have been obtained by adopting condition E, there would then have been difficulties pertaining to contamination, additional cost of post-weld vacuum/inert gas anneal, etc. The overall advantage would thus not have been spectacular enough to warrant its adoption. Considering all the above facts, it can be seen that condition A by itself would be reasonably adequate. It

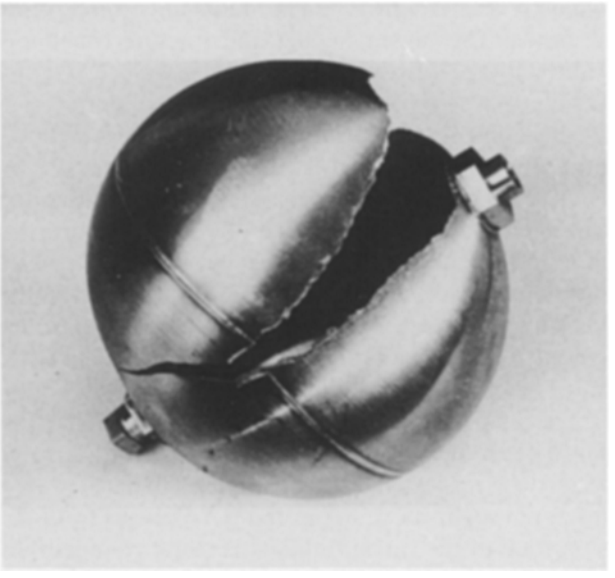

Figure 16 Burst pressure tested gas bottle.

was further checked out in an independent test as follows. An EB welded, 190 mm diameter Ti–6Al–4V spherical gas bottle of 3 mm thickness was burst pressure tested in the as-welded state. The bottle withstood a pressure of 47 MPa as against the design value of 45 MPa and the failure occured in a direction perpendicular to the weld line, as seen in Fig. 16. It therefore is clear that condition A would adequately meet the necessary technical requirements and there was no special reason to go in for any other elaborate conditions. Based on these studies all the Ti–6Al–4V alloy components required for the Indian Space Programme are used in condition A, i.e. the as-EB welded state.

5. Conclusions

1. A sound, narrow, full penetration, single pass, square butt joint with almost parallel cross-section could be prepared from 20 mm thick Ti–6Al–4V plate without any filler wire using an accelerating voltage of 150 kV, a beam current of 68 mA and a travel speed of 125 cm min^{-1}.

2. The fusion zone in the as-welded state exhibits about 90% of the fracture toughness and 95% of the impact toughness of the parent metal at more or less the same UTS values and the electron beam welded Ti–6Al–4V components can be used in the as-welded condition itself.

3. Annealing does not increase the tensile ductility of the welded sample but improves the fracture toughness at both the heat affected zone and the fusion zone.

4. Low temperature stress relieving or ageing carried out subsequent to the welding operation improves the tensile properties but reduces toughness at the fusion zone and heat affected zone.

5. The impact toughness of the HAZ is always found to be more than that of the FZ.

Acknowledgements

The authors are highly indebted to Dr K. Prasada Rao, Assistant Professor, Department of Metallurgy, Indian Institute of Technology, Madras, for critically going through the manuscript and for offering valuable suggestions. The authors also wish to acknowledge their colleagues in the Alloy Processing and Fabrication Section, the Metallographic Laboratory and the Heat Treatment and Welding Section, Materials Testing Section of the Materials and Metallurgy Group, for the assistance and support rendered during the course of preparation of this paper. They also like to place on record their deep sense of gratitude to Shri M. J. Nair, Head, Material Processing Division, Dr K. V. Nagarajan, Head, Materials and Metallurgy Group, and Shri D. Eswaradas, Deputy Director, Materials and Mechanical Systems, for providing all the encouragement and support to complete this work. They also express their sincere thanks to Dr S. C. Gupta, Director, Vikram Sarabhai Space Centre, for according kind permission to publish this work. The assistance given by the Gas Turbine Research Establishment in rendering the necessary help in electron beam welding is also gratefully acknowledged.

References

1. G. THOMAS and M. K. MUKHERJEE, *J. Aero. Soc. India* (1975) 11.
2. G. THOMAS, V. RAMACHANDRA, BHANU PANT, K. V. NAGARAJAN, B. K. SARKAR and R. VASUDEVAN, *Welding J.* (1989) 336_s.
3. M. L. KOHN, G. E. FAULKNER and G. W. BAUER, *Metal Prog.* (1957) 82.
4. L. E. STARK, L. J. BARTLO and H. G. PORTER, *Welding J.* (1962) 805.
5. D. R. MITCHELL and N. G. PEGIE, *Welding Res. Suppl.* (1967) 193_s.
6. Y. OBATA, Y. MORL and K. AOKI, in "Proceedings of the 5th International Conference on Titanium", 1984, Vol. 2 p. 807.
7. E. F. VAUGHAN, in "Proceedings of the Fourth International Conference on Titanium", 1980, Vol. 4, p. 2423.
8. S. M. GUREVICH, O. K. NAZARENKO, V. M. SAMKOV, V. E. LOKSHIN and A. D. SHEVELEV, *ibid.* Vol. 4, p. 2347.
9. A. DURCOT and S. A. SCIAKY, in "Proceedings of the Third International Conference on Titanium", 1976, Vol. 2, p. 1245.
10. K. BORGGREEN and I. WILSON, *Welding J.* (1980) 1_s.
11. R. P. SIMPSON and K. C. WA, "Microstructure–Property Control with Postweld Heat Treatments in Ti-6Al-4V-2 Sn".
12. G. THOMAS, PhD Thesis, Department of Metallurgical Engineering, IIT, Madras (1990).
13. "ASME Boiler and Pressure Vessel Code", Section 8, part UW, p. 79.
14. J. C. CHESTNUTT, C. G. RHODES and J. C. WILLIAMS, in "Fractography–Microscopic Cracking Processes", ASTM STP 600 (American Society for Testing Materials, 1976) p. 99.
15. R. P. SIMPSON, C. M. PIERCE and K. C. WU, in "Titanium Science and Technology", edited by R. I. Jafee and H. M. Burte, Vol. 1 (1973) p. 553.

Received 9 January 1992
and accepted 29 November 1992